



# Phycoremediation of lithium ions from aqueous solutions using free and immobilized freshwater green alga *Oocystis solitaria*: mathematical modeling for bioprocess optimization

Noura El-Ahmady El-Naggar<sup>1</sup> · Ragaa A. Hamouda<sup>2,3</sup> · Nashwa H. Rabei<sup>3</sup> · Ibrahim E. Mousa<sup>4</sup> · Marwa Salah Abdel-Hamid<sup>3</sup>

Received: 15 January 2019 / Accepted: 16 April 2019 / Published online: 9 May 2019  
© Springer-Verlag GmbH Germany, part of Springer Nature 2019

## Abstract

Lithium is registered as a serious pollutant that causes environmental damage to an irrigation water supply. Freshwater green alga (*Oocystis solitaria*) was studied for its potential to remove lithium ions from aqueous solutions. The Plackett–Burman design was applied for initial screening of six factors for their significances for the removal of lithium from aqueous solutions using *Oocystis solitaria* cells. Among the variables screened, pH, lithium concentration, and temperature were the most significant factors affecting lithium removal. Hence, the levels of these significant variables were further investigated for their interaction effects on lithium removal using the Box–Behnken statistical design. The optimum conditions for maximum lithium removal from aqueous solutions by *Oocystis solitaria* were the initial lithium concentration of 200 mg/L, contact time of 60 min, temperature of 30 °C, pH 5, and biomass of *Oocystis solitaria* cells of 1 g/L with agitation condition. Under the optimized conditions, the percentage of maximum lithium removal was 99.95% which is larger than the percentage of lithium removal recorded before applying the Plackett–Burman design (40.07%) by 2.49 times. The different properties of *Oocystis solitaria*, as an adsorbent, were explored with SEM and via FTIR analysis. The spectrum of FTIR analysis for samples of *Oocystis solitaria* cells before lithium biosorption showed different absorption peaks at 3394 cm<sup>-1</sup>, 2068 cm<sup>-1</sup>, 1638 cm<sup>-1</sup>, 1398 cm<sup>-1</sup>, 1071 cm<sup>-1</sup>, and 649 cm<sup>-1</sup> which has been shifted to 3446 cm<sup>-1</sup>, 2924 cm<sup>-1</sup>, 1638 cm<sup>-1</sup>, 1384 cm<sup>-1</sup>, 1032 cm<sup>-1</sup>, and 613 cm<sup>-1</sup>, respectively, after lithium biosorption by the alga. The treatment of aqueous solution containing lithium with *Oocystis solitaria* cells immobilized in alginate beads removed 98.71% of lithium at an initial concentration of 200 mg/L after 5 h. Therefore, *Oocystis solitaria* may be considered as an alternative for sorption and removal of lithium ions from wastewaters.

**Keywords** *Oocystis solitaria* · Biosorption of lithium · Plackett-Burman design · Box–Behnken design · Characterization · Immobilization · SEM · FTIR

---

Responsible editor: Philippe Garrigues

**Electronic supplementary material** The online version of this article (<https://doi.org/10.1007/s11356-019-05214-x>) contains supplementary material, which is available to authorized users.

✉ Noura El-Ahmady El-Naggar  
nouraelahmady@yahoo.com

<sup>1</sup> Department of Bioprocess Development, Genetic Engineering and Biotechnology Research Institute, City of Scientific Research and Technological Applications, New Borg El-Arab City, Alexandria 21934, Egypt

<sup>2</sup> Department of Biology, Faculty of Sciences and Arts - Khulais, University of Jeddah, Jeddah, Saudi Arabia

<sup>3</sup> Department of Microbial Biotechnology, Genetic Engineering and Biotechnology Research Institute, University of Sadat City, Menoufya Governorate 22857, Egypt

<sup>4</sup> Department of Environmental Biotechnology, Genetic Engineering and Biotechnology Research Institute, University of Sadat City, Menoufya Governorate 22857, Egypt

## Introduction

In recent years, there has been growing concern for ecological effects and public health impacts associated with environmental pollution by metals. Contamination of soil with lithium has been increased in recent years due to the high use and disposal of lithium-based products. It is probable that lithium is one of the metals that has recently become a serious environmental contaminant. Lithium is a highly reactive element; it is the lightest alkali metal and can be toxic except when given in tiny amounts. Lithium is naturally present at small concentrations in fresh water (0.07–40 µg/L), seawater (170–190 µg/L), sediment (56 mg/kg), soil (3–350 mg/kg), and Earth's crust (20–60 mg/kg) (Wedepohl 1995). It is present in trace amounts in numerous plants, plankton, and invertebrates at concentrations of 69 to 5760 parts per billion; its functions are uncertain. Lithium bioaccumulation by marine organisms is much higher than terrestrial organisms (Chassard-Bouchaud et al. 1984).

Lithium and its compounds are used in numerous industrial applications, including heat-resistant glass and ceramic industries; flux additives for iron, steel, and aluminum production; manufacture of high-performance grease lubricants, rocket propellants, lithium batteries, and lithium-ion batteries; and production of pharmaceuticals and nuclear fusion furnace (Miyai et al. 1978; Kaneko and Takahashi 1990). Lithium salts, especially the carbonate ( $\text{Li}_2\text{CO}_3$ ), are the drug of choice for the treatment of manic–depressive disorders (Grandjean and Aubry 2009) and in the treatment of other psychiatric conditions (Léonard et al. 1995).

Lithium is recorded as a dangerous pollutant because it reacts with water to produce the caustic lithium hydroxide and hydrogen (Furr 2000). Lithium concentration entering irrigation water supplies should be  $\leq 2.5$  mg/L (Kjølholt et al. 2003). Lithium has numerous effects on humans and on other organisms (Aral and Vecchio-Sadus 2008). The entry of lithium metal into the food chain with possible biological magnification can pose a serious risk to humans. Lithium carbonate can produce multiple toxic symptoms including glyco-gen synthesis, hematopoiesis, thyroid abnormalities (presenting mainly as hypothyroidism and goiter), hair loss, decrease in food taste, weight gain, stomach and gastrointestinal disturbances, edema, hand tremor (Kato et al. 1996), diarrhea, dry mouth, excessive saliva, polyuria, central nervous system and renal tubular damages (Aral and Vecchio-Sadus 2008; Grandjean and Aubry 2009), and sometimes coma and death (Litovitz et al. 1994). Lithium causes disturbances in the invertebrate's (Léonard et al. 1995) and rat embryo's developments (Klug et al. 1992). Lithium preferentially affects activities of  $\text{Mg}^{2+}$ -containing enzymes (Birch 1988). It competes with  $\text{Mg}^{2+}$  and binds selectively to DNA and impairs DNA synthesis (Kuznetsov et al. 1971; Becker and Tyobeka 1990). Therefore, the cleaning up of lithium contamination in the

environment is an important subject particularly in water purification technology (Tsuruta 2005).

Conventional methods applied for the recovery of lithium from aqueous solutions include adsorption (ion exchange), coprecipitation as lithium aluminate, and solvent extraction. However, these methods have several limitations. Sometimes, these methods are ineffective to separate lithium or concentrate in trace concentrations. Some methods that use ion exchange resins to recover lithium have the potential to pollute the environment (Tsuruta 2005; Çicek et al. 2018). However, there is little information on lithium removal using microorganisms. Biosorption is a promising alternative biological technique for treatment of wastewater that uses low-cost biological materials for removal of toxic metal ions (Volesky 2003). Biosorption of lithium using microorganisms is environmentally friendly, cost-effective, and highly efficient in diluted effluents. It has been known for several decades that various green microalgae have proven properties that could be used for bioremediation of metal pollution (Priyadarshani et al. 2011; Ajayan et al. 2011). The biomass of living algae exhibits an affinity to metal cations because of its negative surface charge. The metal cations enter algal cells either by active transport or by endocytosis through chelating proteins. Subsequently, they are usually transported by intracellular protein carriers (Kastanek et al. 2015).

The objectives of this study were to investigate the potential of the unicellular green alga, *Oocystis solitaria*, as a cost-effective biosorbent for the removal of lithium ions from aqueous solutions; to optimize lithium ions removal; and to characterize the algal surface before and after the biosorption process. In addition, the immobilized *Oocystis solitaria* biomass was used in lithium removal.

## Materials and methods

### Isolation and cultivation of alga

*Oocystis solitaria* is a green alga, isolated from a water sample collected from the Nile River, Egypt. The algal purification was performed according to Andersen (2005), and the green alga was identified according to Philipose (1967). *Oocystis solitaria* was grown in axenic cultures at  $24 \pm 2$  °C under a continuous illumination intensity of 3600 lux in a 20-L bottle containing 12 L of BG-11 medium (Rippka et al. 1979) for the 12-day incubation period. The alga was harvested and filtered by filter paper, and then the fresh biomass was used in biosorption experiments.

### Preparation of lithium solutions

Lithium solutions were prepared by dissolving lithium sulfate ( $\text{Li}_2\text{SO}_4$ ) in distilled water) 100 mL to attain the required

concentrations (25–300 mg/L). The initial pH of each concentration was adjusted with 0.1 N H<sub>2</sub>SO<sub>4</sub> or 0.1 N NaOH to the needed pH value.

### Selection of significant variables for lithium removal by the Plackett–Burman design

The Plackett–Burman design (PBD) (Plackett and Burman 1946) is an effective method used for identifying the variables that have significant effects on the process. In this study, the 12-trial PBD was used to screen and assess the effect of the selected six factors either positively or negatively on lithium removal efficiency and to select the significant variables affecting lithium removal. The six independent variables including contact times (60 min or 180 min), initial concentration of lithium (25 mg/L or 200 mg/L), and the physical parameters such as pH level (4 or 7), biomass concentration (1 g/L or 4 g/L), temperature (25 °C or 50 °C), and static or agitation condition were investigated at low (–) and high (+) levels. For each run, the lithium removal was measured and calculated in terms of percentage (%) (Choudhary et al. 2011).

The PBD is based on the first-order model

$$Y = \beta_0 + \sum \beta_i X_i \tag{1}$$

where  $Y$  is the experimental lithium removal percentage,  $X_i$  is the level of each independent variable,  $\beta_0$  is the model intercept, and  $\beta_i$  is the linear coefficient.

*Oocystis solitaria* cells were thoroughly mixed in Erlenmeyer flasks with the lithium solution. The suspensions were kept under specific conditions. After each contact time interval (60 min or 180 min), the residual concentration of lithium in the solution was quantified by using inductively coupled plasma atomic emission spectroscopy (ICP-AES) (Thermo Scientific).

### Optimization of lithium removal by the Box–Behnken design

The experimental Box–Behnken design (BBD) (Box and Behnken 1960) is a response surface methodology used to estimate the optimal levels of the significant independent variable that bring out maximum lithium removal, the individual and interaction effects between the selected process variables affecting lithium removal by *Oocystis solitaria*. Three factors with the highest confidence levels were selected for further optimization using the Box–Behnken design based on the experimental Plackett–Burman design results. These factors were pH ( $X_1$ , 5–9), lithium concentration ( $X_2$ , 100–300 mg/L), and temperature ( $X_3$ , 30–60 °C). Design-Expert software (version 7) for Windows was employed to generate the Box–Behnken design with 15 different experiments and three center points. The significant variables were assessed at three

coded levels (–1 for low, 0 for middle, and +1 for high levels).

To correlate the relationship between the lithium removal percentage ( $Y$ ) and the significant three factors and for predicting the optimal factor levels, the following second-order polynomial equation was used:

$$Y = \beta_0 + \sum_i \beta_i X_i + \sum_{ii} \beta_{ii} X_i^2 + \sum_{ij} \beta_{ij} X_i X_j \tag{2}$$

where  $Y$  is the predicted lithium removal percentage,  $X_i$  is the coded levels of independent variables,  $\beta_0$  is the regression coefficients,  $\beta_{ij}$  is the interaction coefficients,  $\beta_i$  is the linear coefficient, and  $\beta_{ii}$  is the quadratic coefficients.

Trials were performed in triplicates, and intermediate values were given. Three additional confirmation experiments were conducted to verify the model precision.

### Statistical analysis of the data

Design-Expert software (version 7) and Minitab software were used for the experimental designs and statistical analysis, and Statistica software (version 8.0) (StatSoft Inc., Tulsa, USA) was used to plot the 3-D surface plots.

### Lithium quantification by ICP-AES

Lithium concentrations in the solutions were determined by means of ICP-AES (Thermo Scientific, Germany) according to the method described by El-Naggar et al. (2018a). High pure acids and certified reference materials from Merck (Darmstadt, Germany) were included in the analyses through application of QA/QC program according to specification of ISO 17025. The recovery of metals was within the certified limits as 10 ppb to 1000 ppb. To get the final concentration, the solution was diluted with 0.1 mM H<sub>2</sub>NO<sub>3</sub> and the final dilution factors were used (American Public Health Association (APHA) 2005). The reagent blanks in water were below the limit of detection which is 2.82 ppb. Both the initial and residual concentrations were quantified, and the losses of positive control after filtration did not exceed 0.1% of the examined element concentrations. The acidified samples were filtered through disposable 0.2-µm PTFE syringe filters (DISMIC-25HP; Advantec, Tokyo, Japan) into 10 mL Teflon tubes. The membrane filters were washed with the equal sample volume of Li-free water. All the analyses were performed in triplicate.

The efficiency of *Oocystis solitaria* to remove lithium ions from aqueous solutions was calculated quantitatively by using the following equation:

$$\text{Removal efficiency (\%)} = \frac{C_i - C_f}{C_i} \times 100 \tag{3}$$

where  $C_f$  is the residual lithium ions concentration (mg/L) and  $C_i$  is the initial lithium ions concentration (mg/L). All determinations of lithium ions in the solutions were carried out in triplicates, and the determination of lithium removal is an average of three trials.

### Fourier transform infrared spectroscopy

Fourier transform infrared (FTIR) analysis was performed according to the method of El-Naggar et al. (2018b) to confirm the presence of functional groups on the surfaces of *Oocystis solitaria* cells before and after lithium biosorption.

### Scanning electron microscopy

To assess the change in the surface morphology of the algal cells before and after lithium removal, the dry *Oocystis solitaria* biomass samples were gold coated and examined under the electron microscope (Oxford X-Max 20) with different magnifications at 20 kV.

### Immobilization of *Oocystis solitaria* in alginate beads and its application in lithium removal

Immobilized microalgae have been used in a variety of bioprocesses such as the removal of metal ions. The capacity of *Oocystis solitaria* cells for lithium ions biosorption from aqueous solution was determined using a separating funnel packed with immobilized *Oocystis solitaria* cells in sodium alginate beads. Sodium alginate solution (4%) was prepared by adding 4 g sodium alginate to 100 mL of distilled water and well mixed with continuous stirring for better dissolution at 60 °C for 30 min (Kumar and Saramma 2012). After cooling, 1 g of *Oocystis solitaria* cells was added with continuous stirring for 5 min at room temperature.

The beads were obtained by dropping the suspension of cells and sodium alginate mixture using a 3-mL syringe in 2.5%  $\text{CaCl}_2$  solution (cold and sterile) in sterile condition at room temperature with gentle stirring. The obtained beads were spherical with an average diameter of  $1.5 \text{ mm} \pm 0.2 \text{ mm}$ . To remove the unreacted  $\text{CaCl}_2$ , the beads were washed several times with sterile distilled water, and to harden and stabilize the beads, they were stored at 4 °C overnight in sterile distilled water. As a control, sodium alginate beads were prepared without incorporation of *Oocystis solitaria* cells. A 100-mL separating funnel packed with alginate–algal beads was used to perform the biosorption experiment and eluted with lithium ions solution (200 mg/L). Five-milliliter aliquots were collected regularly (every 30 min for up to 5 h) at a flow rate of 3 mL/min and analyzed for lithium quantification. The absorption capacity of *Oocystis solitaria* for lithium ions was

calculated by the difference between lithium solution concentrations before and after absorption.

## Results and discussion

A variety of toxic organic (such as industrial solvents, insecticides, dyes, and pesticides) as well as inorganic (such as fertilizers and metals) pollutants represents an important environmental problem because of their toxic effects and their accumulation throughout the food chain. Metal ions were one of the biggest water pollution problems. Many traditional methods of decontamination have been developed but have not been effective due to economic and technical constraints. A variety of absorbents was used to remove pollutants (Table 1). Throughout the world, there is an ongoing interest in developing promising new, efficient, and cheaper technologies for the efficient destruction and removal of pollutants. Among them is cost-effective and environmentally friendly phycoremediation, involving the use of algae to remove pollutants from the environment.

The process of metal biosorption from aqueous solutions is significantly influenced by several variables including type and biomass concentrations (Li and Tao 2015) and physico-chemical factors (Park et al. 2010) like temperature, pH, dissolved oxygen, initial metal concentration, and contact time. Optimization of metal biosorption process using the traditional one-factor-at-a-time approach, which varies only one variable at a time while keeping all other variables at a constant level, is difficult, laborious, time-consuming, and expensive. In addition, it ignores the effects of interactions between different variables, leading to misinterpretations of the results. Therefore, these defects can be eliminated by optimizing all the variables collectively by using statistical experimental designs such as the Plackett–Burman design and response surface methodology (El-Naggar et al. 2013; El-Naggar 2015).

These statistical designs can be conducted on several steps of an optimization process. The variables could be screened for, firstly, the identification of the significant variables and, secondly, the optimization of the significant variable levels (Nawani and Kapadnis 2005). The statistical experimental designs have many advantages over the traditional method, since the interactions among the process variables can be studied. These methods are suitable for experiments involving multiple variables and are less time-consuming because fewer experiments are performed (Chang et al. 2006; Banik et al. 2007).

### Screening of process variables affecting the biosorption of lithium by *Oocystis solitaria* using the Plackett–Burman design

The effects of different process variables such as pH, contact time, biomass concentrations, temperature, dissolved oxygen,



**Table 1** A variety of adsorbents used to remove pollutants

Pollutant	Adsorbent	References
Toxic metal ions in waste water (Cd, Pb, Cr, Cu, Co, Hg, Ni, Zn, Se)	Various biomass of plant and microbial origin	Gupta et al. (2015)
Chrysoidine Y (hazardous azo dye)	Bottom ash and de-oiled soya	Alok et al. (2010)
Dye–tartrazine	Titanium dioxide	Gupta et al. (2011)
Methylene blue and methyl orange	ZnO/CuO nanocomposite	Saravanan et al. (2013a)
Methylene blue and methyl orange	ZnO nanorods	Saravanan et al. (2013b)
Methylene blue and methyl orange	Hg-doped ZnO nanorods	Saravanan et al. (2013c)
Organic and inorganic pollutants	Carbon nanotubes and fullerene	Gupta and Saleh (2013)
Rhodamine B	Carbon nanotube/tungsten oxide	Saleh and Gupta (2011)
Metals, dyes, phenols, and other organic compounds	Rice husk and rice husk ash	Ahmaruzzaman and Gupta (2011)
Methyl orange dye	Mesoporous carbon	Mohammadi et al. (2011)
Methyl orange and methylene blue	ZnO/Ag/CdO nanocomposite	Saravanan et al. (2015)
Methylene blue and Safranin-O	Fe <sub>3</sub> O <sub>4</sub> NPs	Ghaedi et al. (2015)
Phenol	Pyrolyzed sewage sludge	Gupta et al. (1998)
Phenolic compounds	Activated carbons	Gupta et al. (2014b)
Degradation of aqueous methylene blue solution	CeO <sub>2</sub> , V <sub>2</sub> O <sub>5</sub> , CuO, CeO <sub>2</sub> /V <sub>2</sub> O <sub>5</sub> , and CeO <sub>2</sub> /CuO nanocatalysts	Saravanan et al. (2013e)
Methyl orange, methylene blue, rhodamine 6G, and rhodamine B	ZnO/Ag nanocomposite	Saravanan et al. (2013d)
Nitrophenol compounds	Fe@Au bimetallic nanoparticles	Gupta et al. (2014a)
Methylene blue and methyl orange	ZnO/ $\gamma$ -Mn <sub>2</sub> O <sub>3</sub> nanocomposite	Saravanan et al. (2014a)
Chromium	Activated carbons	Gupta et al. (2013)
Methyl orange and methylene blue	ZnO	Saravanan et al. (2013f)
Organic pollutants	Vanadium pentoxide V <sub>2</sub> O <sub>5</sub> /ZnO	Saravanan et al. (2014b)
Methyl orange	Carbon nanotubes and titanium dioxide	Saleh and Gupta (2012)
1-(2-Ethoxyphenyl)-3-(3-nitrophenyl) triazene	Multiwalled carbon nanotubes	Khani et al. (2010)

and metal concentrations on the lithium biosorption have been studied. The Plackett–Burman design was used to identify the most significant process variables for maximum removal of lithium from aqueous solutions by using *Oocystis solitaria* cells. *Oocystis solitaria* is a small, unicellular green alga with ovoid or lemon-shaped cells (Fig. S1). The Plackett–Burman design experiment was conducted in 12 trials ( $N = 12$ ) with two levels (high and low levels) for each independent variable to study the effect of different process variables on the percentage of lithium removal. Caution must be exercised while setting the high and low levels, since the small variation in the level may not show any effect, and the large difference in the level of a sensitive variable can hide other variables (Greasham and Inamine 1986). The experimental Plackett–Burman design matrices selected for the screening of significant variables along with the corresponding lithium removal percentages and residuals are shown in Table 2. The Plackett–Burman design experiments showed a markedly wide variation in lithium removal % (Table 2); this variation reflected the importance of the optimization process to attain maximum lithium removal. There was a wide variation in lithium

removal percentages ranging from 89.58 to 97.14% throughout the different trials of the Plackett–Burman design experiment. This variation highlighted the importance of the optimization process to attain higher lithium removal percentage.

### Multiple regression analysis and analysis of variance

In order to evaluate the relationship between lithium removal percentages and the independent process variables, the data that were analyzed using multiple regression statistical analysis and the analysis of variance (ANOVA) are represented in Tables 3 and 4. The estimated main effect of each examined variable on lithium removal percentage was calculated and is illustrated in Table 3 and Fig. 1a. If the estimated main effect was positive, a higher level was required during further optimization studies. The large positive or negative estimated main effect indicates that the process variable has a large impact on lithium removal percentage, while the near-zero effect means that the process variable has little or no effect on lithium removal. The percentages of contribution of different variables are shown in Table 3.

**Table 2** Twelve-trial Plackett–Burman experimental design for evaluation of independent variables with coded and actual levels along with the observed and predicted values of lithium removal by *Oocystis solitaria*

Run no.	Coded and actual levels of independent variables											Lithium removal (%)		Residuals	
	Time (min)	Lithium conc. (mg/L)		pH	Temperature (°C)		Biomass (g)	Agitation–static		Actual value	Predicted value				
1	-1	60	-1	25	-1	4	+1	50	+1	4	+1	Agitation	95.1	95.31	-0.30
2	-1	60	-1	25	+1	7	+1	50	+1	4	-1	Static	96.17	95.99	0.18
3	-1	60	+1	200	+1	7	+1	50	-1	1	+1	Agitation	94.75	99.78	-0.32
4	+1	180	-1	25	+1	7	+1	50	-1	1	+1	Agitation	96.43	95.99	0.44
5	+1	180	-1	25	-1	4	-1	25	+1	4	+1	Agitation	92.53	91.81	0.72
6	-1	60	+1	200	-1	4	-1	25	-1	1	+1	Agitation	95.55	94.98	0.57
7	+1	180	+1	200	-1	4	+1	50	-1	1	-1	Static	96.43	96.09	0.34
8	+1	180	+1	200	+1	7	-1	25	+1	4	+1	Agitation	95.77	96.89	-1.12
9	-1	60	-1	25	-1	4	-1	25	-1	1	-1	Static	89.58	90.57	-0.99
10	+1	180	-1	25	+1	7	-1	25	-1	1	-1	Static	91.82	91.87	-0.05
11	+1	180	+1	200	-1	4	+1	50	+1	4	-1	Static	96.36	96.70	-0.34
12	-1	60	+1	200	+1	7	-1	25	+1	4	-1	Static	97.14	96.28	0.86

The -1 sign corresponds to the minimum value, and the +1 sign corresponds to the maximum value of the input parameter range

Different process variables were screened at a confidence level of 95%. If the variable showed significance at or above the confidence level of 95%, it indicated that the variable was effective in lithium removal %. Also, the lower probability value ( $P$  value < 0.05) indicates that the process variable has a significant effect on the lithium removal. The results showed that lithium concentration ( $B$ ) with a very low probability value (0.002) was the most significant factor affecting lithium removal percentage by *Oocystis solitaria* which is followed in significance by temperature ( $D$ ) and then pH ( $C$ ) with  $P$  values of 0.003 and 0.018, respectively. Also, the results revealed that agitation/static ( $F$ ), biomass ( $E$ ), and contact time ( $A$ ) are insignificant factors with lower effects (1.2, 0.62, and -0.6, respectively) and lower contribution percentages (11.516, 5.950, and 5.758, respectively). The statistical significance of the model was determined by the results of ANOVA which showed that the model was highly significant as was

demonstrated by Fisher’s  $F$  test of 13.586, the  $t$  statistic of 347.628, and a very low  $P$  value of 0.006.

The coefficient of each factor represents the extent to which this factor affects the removal of lithium. Moreover, it was clear that agitation/static, biomass, temperature, pH, and the concentration of lithium had positive effects on lithium removal (the values of coefficients are 0.60, 0.31, 1.46, 0.94, and 1.60, respectively). The contact time is an insignificant variable and has a negative effect on the removal of lithium (the value of coefficient = -0.30) which means that low contact time levels can have a positive effect on lithium removal.

The values of determination coefficient ( $R^2$ ) are usually used to verify the quality of the model and to provide a measure of the variation in observable response values that can be explained by experimental factors. The value of  $R^2$  is always between 0 and 1. When the value of  $R^2$  is close to 1, the model is stronger and the response is best expected. In our study, the

**Table 3** Regression statistics for the experimental results of the Plackett–Burman design used for lithium removal by *Oocystis solitaria*

Source	df	Coefficient	Effect	$t$ statistics	$P$ value	Confidence level (%)	Contribution (%)
Intercept		95.19		347.628	0.000*	100	
Contact time ( $A$ )	1	-0.30	-0.6	-1.086	0.327	67.3	5.758
Lithium conc. ( $B$ )	1	1.60	3.2	5.834	0.002*	99.8	30.710
pH ( $C$ )	1	0.94	1.88	3.448	0.018*	98.2	18.042
Temperature ( $D$ )	1	1.46	2.92	5.317	0.003*	99.7	28.023
Biomass ( $E$ )	1	0.31	0.62	1.129	0.310	69	5.950
Agitation–static ( $F$ )	1	0.60	1.2	2.206	0.078	92.2	11.516

$R = 0.9707$ ;  $R^2 = 0.9422$ ; adjusted  $R^2 = 0.8729$ ; PRESS = 25.9122

df degree of freedom,  $P$  level of significance

\*Significant values

**Table 4** Analysis of variance (ANOVA) for the experimental results of the Plackett–Burman design

	df	SS	MS	F	Significance F
Regression	6	73.344	12.224	13.586	0.006*
Residual error	5	4.499	0.900		
Total	11	77.843			

df degree of freedom, F Fisher’s function

\*Significant values

$R^2$  value is 0.9422 which means that the variation in the lithium removal of 94.22% can be explained by the model used. The current  $R^2$  value of 0.9422 indicates a better relationship between the observed and the expected response values. In

addition, the highest value of the adjusted  $R^2$  (0.8729) (Table 3) indicates a high significance level of the model and greater precision in the correlation between the experimental variables and the lithium removal.

The Pareto chart shown in Fig. 1b showed that the concentration of lithium (B) was the most significant factor affecting lithium removal (30.71%) followed by temperature (28.02%), pH (18.04%), agitation/static (11.52%), biomass (5.95%), and then contact time (5.76%).

A first-order polynomial equation that defines the removal percentages of lithium was derived in terms of the independent variables. By neglecting the insignificant terms, the following regression equation was obtained:

$$\text{Lithium removal (\%)} = 95.19 + 1.60 \text{ lithium concentration (mg/L)} + 0.94 \text{ pH} + 1.46 \text{ temperature (}^\circ\text{C)} \quad (4)$$

In a confirmation experiment, to assess the Plackett–Burman accuracy, the expected optimum conditions to attain maximum removal of lithium by *Oocystis solitaria* from aqueous solutions were an initial lithium concentration of 200 mg/L, contact time of 60 min, temperature 50 °C, *Oocystis solitaria* biomass of 1 g/L, and pH 7 with agitation condition. The maximum lithium removal obtained under these optimum conditions was 99.2% which is higher than the percentage of lithium removal obtained prior to application of the Plackett–Burman design (40.07%) by 2.47 times.

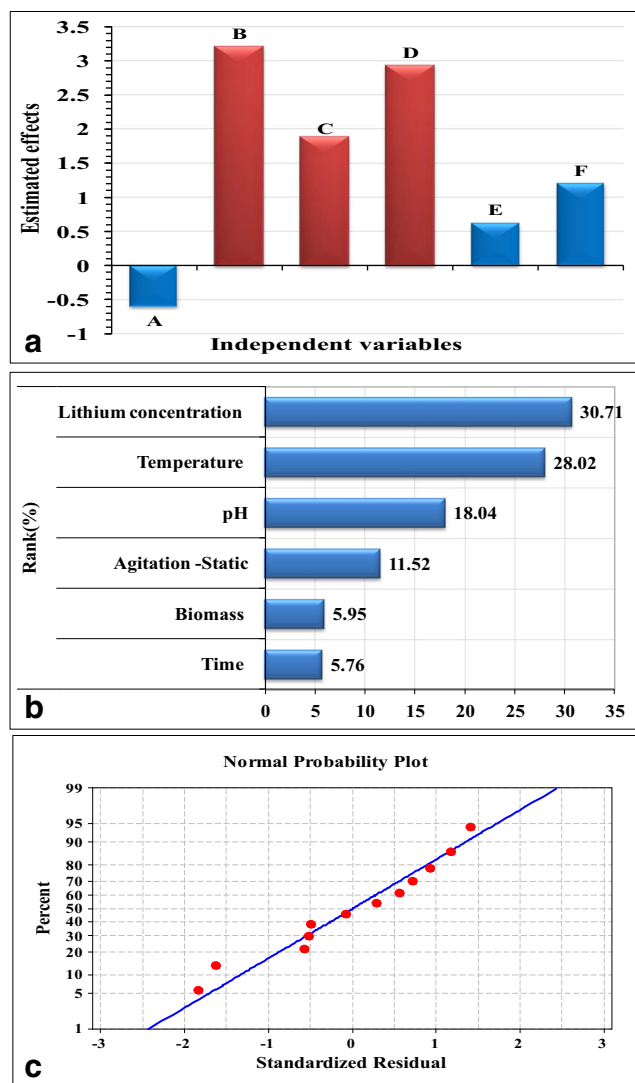


**Fig. 1** a Estimated effects of independent variables. The red color represents the most significant positive independent variables affecting lithium ions biosorption removal. b Pareto chart. c The normal probability plot of the residuals for removal of lithium ions by *Oocystis solitaria* determined by the first-order polynomial equation

### Statistical optimization of lithium removal by *Oocystis solitaria* using the BBD

Based on the results of the Placket–Burman design, the BBD was used to determine the optimal levels of the most significant factors affecting the removal of lithium and also to study their interactions. In this study, a total of 15 experiments with a different combination of pH ( $X_1$ ), the concentration of lithium ( $X_2$ ), and temperature ( $X_3$ ) were performed. Coded and actual levels of the three independent factors are presented in Tables 5 and 6. Contact time with a negative coefficient and the biomass (insignificant factor) were maintained in BBD experiments at their low levels of PBD. The experimental results and the results of theoretically predicted lithium removals along with the residuals are shown in Table 5. Based on the obtained experimental results of the BBD, percentages of lithium removal ranged from 90.24 to 99.95. The highest lithium removal percentage was obtained in trial no. 5 (99.95%) at pH 5, temperature of 30 °C, and lithium concentration of 200 mg/L. While the minimum lithium removal percentage was recorded in trial no. 10 (90.24%) at pH 7, a temperature of 60 °C, and a lithium concentration of 100 mg/L. The predicted lithium removal percentages fit well with those of the experimentally obtained lithium removal percentages.

**Table 5** Box–Behnken design representing the observed and predicted lithium removal % by *Oocystis solitaria*

Standard order	Run	Type	Variables			Lithium removal (%)		Residuals
			$X_1$	$X_2$	$X_3$	Experimental	Predicted	
7	1	Factorial	-1	0	+1	92.6	92.52	0.08
15	2	Center	0	0	0	99.87	99.43	0.44
2	3	Factorial	+1	-1	0	94.6	94.69	-0.09
12	4	Factorial	0	+1	+1	95.57	95.74	-0.17
5	5	Factorial	-1	0	-1	99.95	99.90	0.05
13	6	Center	0	0	0	98.54	99.43	-0.89
6	7	Factorial	+1	0	-1	95.16	95.24	-0.08
14	8	Center	0	0	0	99.89	99.43	0.46
3	9	Factorial	-1	+1	0	97.73	97.64	0.09
11	10	Factorial	0	-1	+1	90.24	90.10	0.14
4	11	Factorial	+1	+1	0	97.44	97.22	0.22
8	12	Factorial	+1	0	+1	95.35	95.40	-0.05
9	13	Factorial	0	-1	-1	97.45	97.28	0.17
1	14	Factorial	-1	-1	0	95.82	96.04	-0.22
10	15	Factorial	0	+1	-1	95.64	95.78	-0.14

## Multiple regression analysis and ANOVA

The experimental Box–Behnken design results were analyzed using multiple regression analysis, and the results of ANOVA are shown in Table 7 and Table S1. The regression model contains three linear ( $X_1$ ,  $X_2$ ,  $X_3$ ), three interaction ( $X_1X_2$ ,  $X_1X_3$ ,  $X_2X_3$ ), and three quadratic ( $X_1^2$ ,  $X_2^2$ ,  $X_3^2$ ) effects (Table 7). Cui et al. (2009) reported that a regression model with an  $R^2$  value greater than 0.9 was considered to be very highly correlated. The present regression model has an  $R^2$  value of 0.9865 which means that the variation in the lithium removal of 98.65% can be explained by the model. In addition, the adjusted  $R^2$  value (0.9621) was too high to confirm the great significance of the model (Table 7). The predicted  $R^2$  indicates how the regression model predicts responses for new experiments successfully. The predicted  $R^2$  value of 0.9400 is in a reasonable agreement with the adjusted  $R^2$  value of 0.9621. This indicates a good adjustment between the observed and predicted values. The adequate precision value of the present model was 22.4905, indicating that the model can be used to navigate the space of design. The PRESS value is 6.31, and the values of mean and standard deviation are 96.39 and 0.53, respectively (Table 7). The low value of the coefficient of variation % (CV = 0.55%) indicates the high precision of the performed experiments (Box et al. 1978).

The statistical significance of the quadratic model was determined by the results of ANOVA which implies that the model is highly significant as was demonstrated by the high  $F$  value of 40.52 and the very low probability ( $P$ ) value of 0.0004 (Table 7). The nonsignificant lack of fit ( $P$  value = 0.9367) indicates that the experimental results obtained were

well fitted with the model. The significance of each coefficient was determined by the  $P$  value as shown in Table 7. Interpretation of the experimental results in Table 7 was dependent on the signs of the variable coefficients and  $P$  values to understand the interactions between the test variables. Fundamentally, interactions between two factors can be either positive or negative on the response. The negative sign indicates an antagonistic effect, but the positive sign indicates a synergistic effect on the response. From  $P$  values, we can see that linear coefficients of  $X_2$  and  $X_3$ , the interaction between  $X_1X_3$  and  $X_2X_3$ , and quadratic effect of  $X_1$ ,  $X_2$ , and  $X_3$  are significant. The interaction between  $X_1$  and  $X_3$  (pH and temperature) and the interaction between  $X_2$  and  $X_3$  (concentration of lithium and temperature) had a significant effect with  $P$  values of 0.0009 and 0.0011, respectively. Furthermore, the  $P$  values indicate that of the three variables examined, the quadratic effect of  $X_3$  ( $X_3^2$ ) had a very significant effect on the removal of lithium by *Oocystis solitaria* ( $P$  value = 0.0002). On the other hand, the linear coefficients of pH and interaction between pH and concentration of lithium are not significant.

Table S1 shows the results of fit summary to determine higher-order polynomial model significant terms and insignificant lack-of-fit test. The results of the fit summary (Table S1) show that the quadratic model is a highly significant model and suitable model that fit the Box–Behnken design of lithium removal by *Oocystis solitaria* with a very low  $P$  value of 0.0004 and nonsignificant lack of fit ( $P$  value = 0.9367). The quadratic model has the highest adjusted and predicted  $R^2$  values of 0.9621 and 0.9400, respectively, and the smallest standard deviation of 0.53.



**Table 6** The actual factor levels corresponding to the coded factor levels chosen for Box–Behnken design experiment

Variable	Variable code	Coded and actual levels		
		− 1	0	1
pH	$X_1$	5	7	9
Lithium conc. (mg/L)	$X_2$	100	200	300
Temperature (°C)	$X_3$	30	45	60

By applying the variable coefficients (Table 7), the second-order polynomial equation that describes the relationship between lithium removal % by *Oocystis solitaria* ( $Y$ ) in terms of pH, the concentration of lithium, and temperature was obtained for predicting the optimal point

$$Y = +99.43 - 0.44(\text{pH}) + 1.03(\text{lithium concentration}) - 1.81(\text{temperature}) + 0.23(\text{pH} \times \text{lithium concentration}) + 1.89(\text{pH} \times \text{temperature}) + 1.79(\text{lithium concentration} \times \text{temperature}) - 1.00(\text{pH})^2 - 2.04(\text{lithium concentration})^2 - 2.67(\text{temperature})^2 \quad (5)$$

**The normal probability plot of the residuals**

Figure 1c shows the normal probability plot (NPP) of the experimental results to verify the adequacy of the model. The predicted values of the model were plotted against the residuals in a way that make the points close to a diagonal

straight line for lithium removal %. Departure from this diagonal line means a deviation from normality. Figure 1c shows that the residuals from the predicted responses follow a normal distribution and close to the diagonal straight line. This means that the model had been validated.

**Contour and 3-D plots**

To determine the optimal levels of the tested variables and their interaction effects upon lithium removal, the 3-D response surface plots and 2-D contour plots for the pairwise combinations of the three variables ( $X_1X_2$ ,  $X_1X_3$ , and  $X_2X_3$ ) were drawn. Lithium removal % was plotted on the Z-axis against two process variables while keeping the other variables at its zero level, as illustrated in Fig. 2.

The 3-D and contour plot in Fig. 2a shows lithium removal as a function of the effects of pH ( $X_1$ ) and lithium concentration ( $X_2$ ), while maintaining temperature ( $X_3$ ) at its zero level (45 °C). It was observed that a relatively higher percentage of lithium removal was high at low and middle levels of pH ( $X_1$ ). But, the percentage of lithium removal was decreased at low and high levels of lithium concentration ( $X_2$ ). The maximum lithium removal percentage was obtained at the middle level of lithium concentration. For optimization of the process parameters, the point prediction option in the software was used. The maximum predicted lithium removal of 99.60% has been obtained at the optimum predicted levels of pH 6.5 and lithium concentration of 220 mg/L at a temperature of 45 °C.

**Table 7** Regression statistics and analysis of variance (ANOVA) for the Box–Behnken design results used for lithium removal % by *Oocystis solitaria*

Source	Coefficient estimate	df	F value	P value probability > F
Model	99.43	9	40.52	0.0004*
$X_1$ (pH)	− 0.44	1	5.53	0.0654
$X_2$ (lithium concentration, mg/L)	1.03	1	30.03	0.0028*
$X_3$ (temperature, °C)	− 1.81	1	91.56	0.0002*
$X_1X_2$	0.23	1	0.76	0.4233
$X_1X_3$	1.89	1	49.93	0.0009*
$X_2X_3$	1.79	1	44.77	0.0011*
$X_1^2$	− 1.00	1	12.92	0.0156*
$X_2^2$	− 2.04	1	53.87	0.0007*
$X_3^2$	− 2.67	1	92.50	0.0002*
Residual	1.42	5		
Lack of fit	0.23	3	0.13	0.9367
Pure error	1.20	2		
Total correlation	105.22	14		

Standard deviation = 0.53; mean = 96.39; CV % = 0.55; PRESS = 6.31;  $R^2 = 0.9865$ ; adjusted  $R^2 = 0.9621$ ; predicted  $R^2 = 0.9400$ ; adequate precision = 22.4905

df degree of freedom, F Fisher’s function, P level of significance

\*Significant values

Figure 2a shows that the initial lithium ions concentration significantly affected the biosorption of its ions. Lithium concentration is one of the most important variables affecting the lithium biosorption. Lithium ions biosorption has been increased with an increasing concentration of lithium ions till the maximum reached. However, increased lithium concentration leads to a gradual reduction in the lithium removal percentage. The maximum metal adsorption at the initial higher concentration of metal ions can be attributed to the fact that all adsorption active sites on the surface of the algal biomass were initially vacant and remain unsaturated which enhances high adsorption of metals initially (El-Sikaily et al. 2007; Aravindhana et al. 2007). Subsequently, with increased metal concentration, the removal rate of metal decreased due to the binding sites available on the surface of algae which has been saturated (Ho et al. 2001). Increasing the concentration of metal ions increases the adsorption capacity of the adsorbent due to increased mass transfer rate (Garg et al. 2008).

The initial pH of the solution has been reported in many studies to be the most important process factor influencing the biosorption of metal ions by biosorbents (Pagnanelli et al. 2003) and affecting the availability of the binding sites to the sorbate resulting in a decrease or increase in metal biosorption (Vijayaraghavan and Yun 2008; Dadrasnia and Ismail 2015). Since the mechanism of the biosorption process is well known to be ion exchange and the pH could affect the net charge and the functional groups on the biosorbent surface, which affects the availability of sorbent binding sites (Romera et al. 2007), protons compete with cations of metal and  $H^+$  for the sorbent binding sites (Dadrasnia and Ismail 2015). Moreover, the pH value affects the metal ion solubility in water (Romera et al. 2007). High alkaline pH value decreases the solubility of metal, resulting in low absorption rate (Kumar et al. 2013). The maximum lithium biosorption was obtained at a pH value of 3–4. The increase in metal biosorption with increasing pH can result due to decreasing competition between metal ions and protons for the same functional groups or due to the low positive charge of the biosorbent, resulting in low electrostatic repulsion between the metal ions and biosorbent surface (Reddad et al. 2002). At pH 5–6, the electrostatic repulsions are reduced between the positively charged metal ions and the adsorbent surface, resulting in increasing the rate of metal removal (Ibrahim 2011; Momcilovic et al. 2011; Hassan et al. 2014). Further, the reduction in the metal ion biosorption rate at higher pH values may be related to the repulsion between the negative charges of the sorbent surface and of anionic species in the solution (Kumar et al. 2006; Esmaili and Beni 2015) or may be attributed to the decreased in the solubility of metals (Kumar et al. 2013). Gupta and Rastogi (2008) stated that higher pH values may affect the number of negatively charged sorbent binding sites, which largely depend on the functional group's dissociation. Our results showed that the maximum

lithium removal was recorded at pH 5. The low biosorption rate of lithium at the alkaline pH value may be associated with an increase in the ability of protons to compete with lithium ions for the alga binding sites.

The 3-D graph and its contour plot (Fig. 2b) describes the relationship between pH ( $X_1$ ), temperature ( $X_3$ ), and lithium removal, while maintaining the concentration of lithium ( $X_2$ ) at its zero level (200 mg/L). An increase in temperature between 30 and 35 °C tends to increase lithium removal. At higher temperatures, lithium removal decreased. It was observed that the maximum percentage of lithium removal clearly supported at low and middle levels of pH ( $X_1$ ). At higher levels of pH, lithium removal percentage could be relatively low. The maximum predicted lithium removal of 100.071% has been obtained at the optimum predicted levels of temperature of 32 °C, pH 5, and lithium concentration of 200 mg/L.

The rate of metal removal increases with an increase in solution temperature by increasing solute kinetic energy and the surface activity (Vijayaraghavan and Yun 2008; Park et al. 2010). Also, the increase in the biosorption rate with the increase of temperature may be attributed to the formation of new adsorption active sites, because of the increase in the rate of metal ion diffusion within the pores of the algae biomass surface as a result of the reduction of solution viscosity (Al-Ashed and Duvnjak 1995) or due to the increase of the surface area available to absorb the metal ions (Saleem et al. 2007). However, at higher temperatures (higher than 45 °C), a decrease in the metal biosorption may occur as a result of physical damage to the biosorbent surface or because of the destruction of some active binding sites (Meena et al. 2005) or because of the weak adaptive forces between the active binding sites of the biosorbent surface and the metal ions (Lian et al. 2009). Conducting the biosorption process at room temperature is always desirable due to the ease of repeating this condition (Vijayaraghavan and Yun 2008).

Three-dimensional and contour plots presented in Fig. 2c show lithium removal as a function of lithium concentration ( $X_2$ ) and temperature ( $X_3$ ), while pH ( $X_1$ ) was kept fixed at zero level (7). An increase in lithium removal was found with an increase of temperature up to 30–35 °C. The increase in lithium removal was observed with increased lithium concentration to the optimal level, and thereafter, the lithium removal has been decreased. The maximum predicted lithium removal was 99.76% at the optimum predicted temperature of 40 °C and the lithium concentration of 205 mg/L at pH 7.

## Verification of the model

The verification of the statistical model and second-order regression equation was conducted by removal of lithium from aqueous solution by using *Oocystis solitaria* under the optimum conditions of 200 mg/L initial lithium concentration, 1

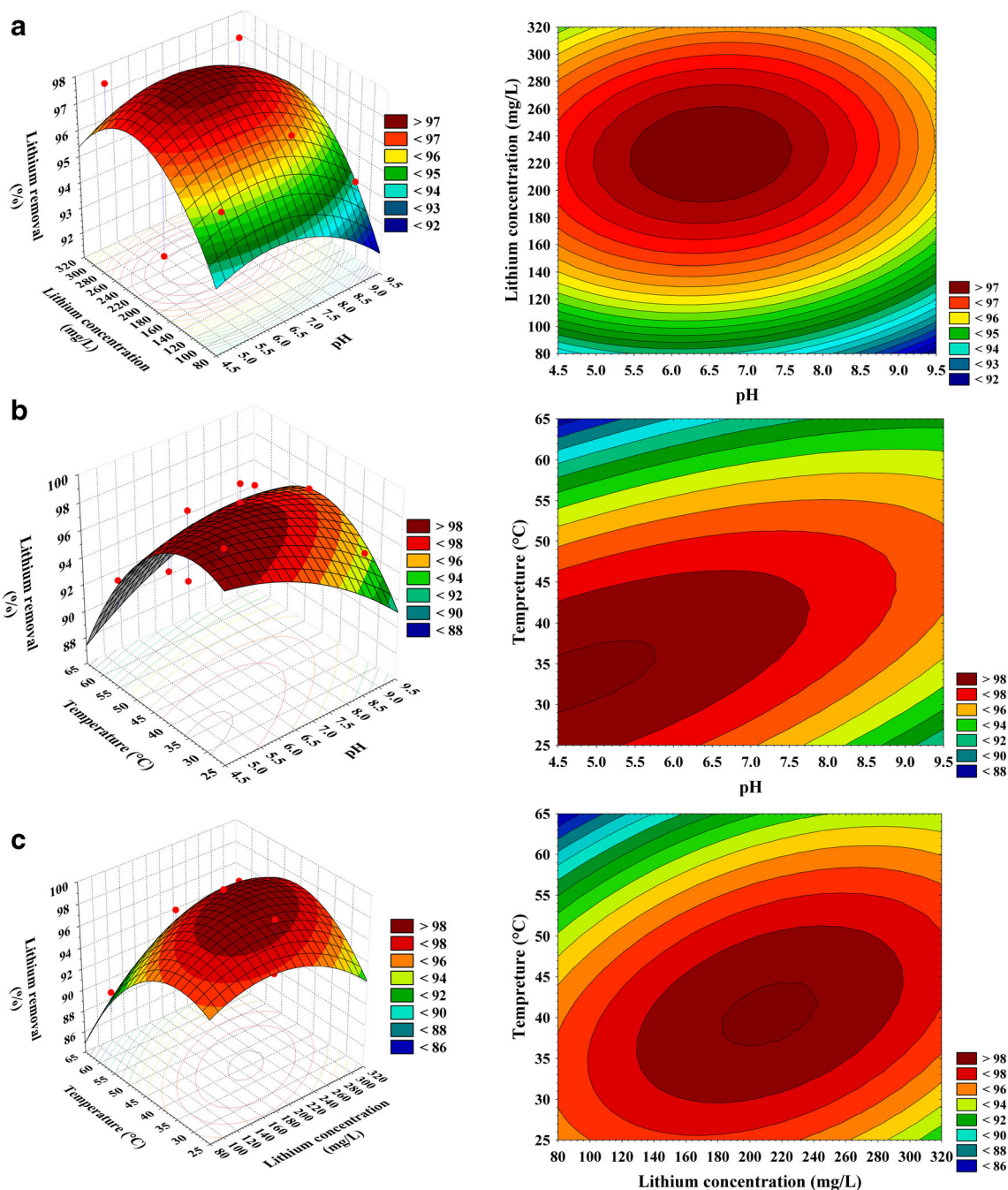


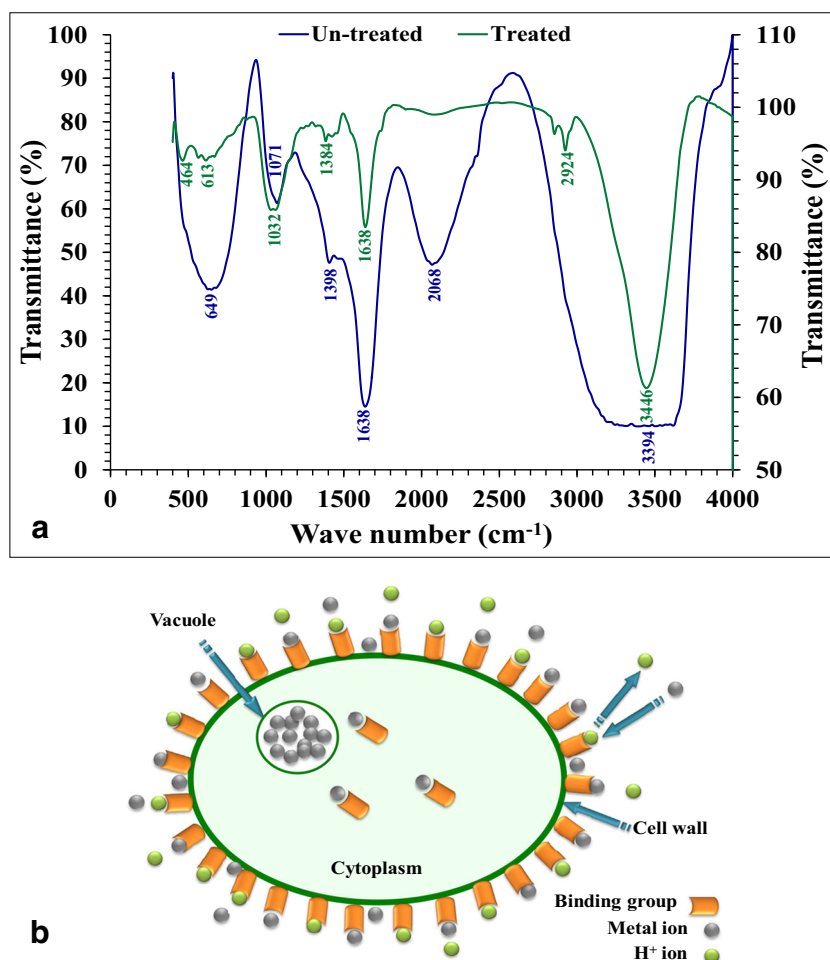
**Fig. 2** a–c Three-dimensional response surface and contour plots of the effects of pH ( $X_1$ ), lithium concentration ( $X_2$ ), and temperature ( $X_3$ ) and their mutual effect on lithium ions removal by *Oocystis solitaria*

g/L *Oocystis solitaria* biomass, and contact time of 60 min at 30 °C and pH 5 with agitation condition. Under these optimized conditions, the experimental percentage of lithium removal was 99.95%. The close relationship between the experimental percentage of lithium removal (99.95%) and predicted value from the model (99.90%) revealed the validity of the model for the optimization of lithium removal under the used conditions.

**FTIR analysis**

The cells of *Oocystis solitaria* were analyzed using FTIR analysis before and after biosorption of lithium, and the FTIR analysis spectra are shown in Table S2 and Fig. 3a. FTIR analysis was performed to detect the variations in the functional groups due to the interaction of metal ions with *Oocystis solitaria* cells. The FTIR analysis spectra of

**Fig. 3** **a** FTIR of *Oocystis solitaria* before and after lithium ions biosorption from aqueous solution. **b** Schematic diagram showing the mechanism of biosorption of metal ions by ion exchange mechanism across the cell surface of an algal cell



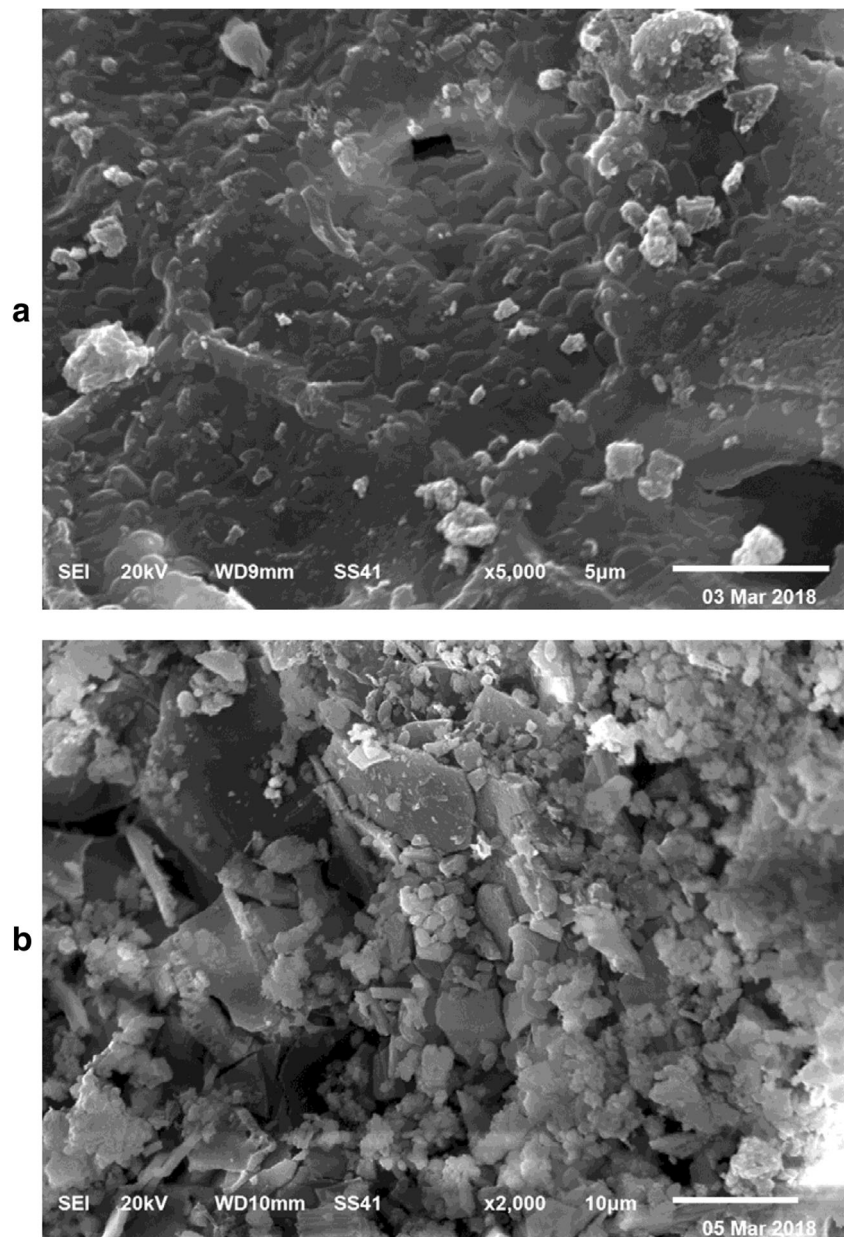
*Oocystis solitaria* cells, before and after biosorption of lithium, were measured within the range of 400–4000  $\text{cm}^{-1}$  wave number (Garg et al. 2008). The Chlorophyta possess cell walls composed of cellulose, xyloglucan, mannans, glucuronan, (1  $\rightarrow$  3)- $\beta$ -glucan, and ulvans (Popper et al. 2011). Different functional groups that act as metal binding sites can be provided by different components of the cell wall. Lithium ions biosorption can occur on the cell surface via the ion exchange mechanism, where the lithium ions binds to the binding sites by replacing one acidic H, and the access of lithium ions to the binding sites of alga surface is improved with increased availability of these binding sites (Fig. 3b).

The spectrum of FTIR analysis for *Oocystis solitaria* cell samples before lithium biosorption showed different absorption peaks at 3394  $\text{cm}^{-1}$ , 2068  $\text{cm}^{-1}$ , 1638  $\text{cm}^{-1}$ , 1398  $\text{cm}^{-1}$ , 1071  $\text{cm}^{-1}$ , and 649  $\text{cm}^{-1}$  which has been shifted to 3446  $\text{cm}^{-1}$ , 2924  $\text{cm}^{-1}$ , 1638  $\text{cm}^{-1}$ , 1384  $\text{cm}^{-1}$ , 1032  $\text{cm}^{-1}$ , and 613  $\text{cm}^{-1}$ , respectively, after lithium biosorption by the alga. One new characteristic absorption peak at 464  $\text{cm}^{-1}$  was observed. The absorption peak before lithium biosorption at 3394  $\text{cm}^{-1}$  wave number is the characteristic absorption peak

of primary amine (N–H) vibration which is shifted by + 52  $\text{cm}^{-1}$  after lithium biosorption by the alga to the sharp peak observed at 3446  $\text{cm}^{-1}$  which is assigned to the –OH or N–H stretching vibration of cellulose (Ghosh and Mittal 1996). Furthermore, during the biosorption process, a large upshift of the peak at 2068  $\text{cm}^{-1}$  to the peak at 2924  $\text{cm}^{-1}$  by + 856  $\text{cm}^{-1}$  has occurred due to the interaction between the *Oocystis solitaria* alga and lithium. The peak at 2068  $\text{cm}^{-1}$  is assigned to the C $\equiv$ N group (Van de Voort et al. 2007) while the peak occurring at 2924  $\text{cm}^{-1}$  is related to the C–H stretching vibration (Janakiraman and Johnson 2015). The strong peak observed at 1638  $\text{cm}^{-1}$  corresponds to the broad O–H stretch (Jackson et al. 2009). The absorption peak before lithium biosorption at 1398  $\text{cm}^{-1}$  is shifted by – 14  $\text{cm}^{-1}$  to the absorption peak at 1384  $\text{cm}^{-1}$ . The peak at 1398  $\text{cm}^{-1}$  wave number corresponds to the COO $^{-}$  symmetric stretching of fatty acids and amino acids and the peak of CH $_3$  bending of protein (Li et al. 2014; Staniszewska-Slezak et al. 2015) while the absorption peak observed at 1384  $\text{cm}^{-1}$  is assigned to the formate ion, HCOO $^{-}$  (Hudson and Moore 2000). Also, during the biosorption process, a shift of the peak at 1071  $\text{cm}^{-1}$  to the peak which appeared at 1032  $\text{cm}^{-1}$  by – 39  $\text{cm}^{-1}$  has occurred



**Fig. 4** SEM micrograph of *Oocystis solitaria* **a** before and **b** after adsorption of lithium ions from aqueous solution



due to the interaction between the *Oocystis solitaria* alga and lithium. The peak at  $1071\text{ cm}^{-1}$  is assigned to the C–O stretching vibration (Gunasekaran and Abitha 2005), and the peak which appeared at  $1032\text{ cm}^{-1}$  corresponds to the O–CH<sub>3</sub> stretching (Kudre et al. 2017). In algal cells before biosorption of lithium, the characteristic absorption peak at  $649\text{ cm}^{-1}$  which is assigned to B–O bending vibrations (Zahariev et al. 2017) is shifted by  $-36\text{ cm}^{-1}$  after biosorption of lithium to the peak at  $613\text{ cm}^{-1}$  assigned to the C=C–C stretching vibration (Devi and Gayathri 2010), whereas the small bands appearing at  $464\text{ cm}^{-1}$  correspond to the Si–O–Si asymmetric stretching mode (Salem et al. 2015).

FTIR analysis confirmed that the main functional groups on the cell surface of *Oocystis solitaria* that are involved in the

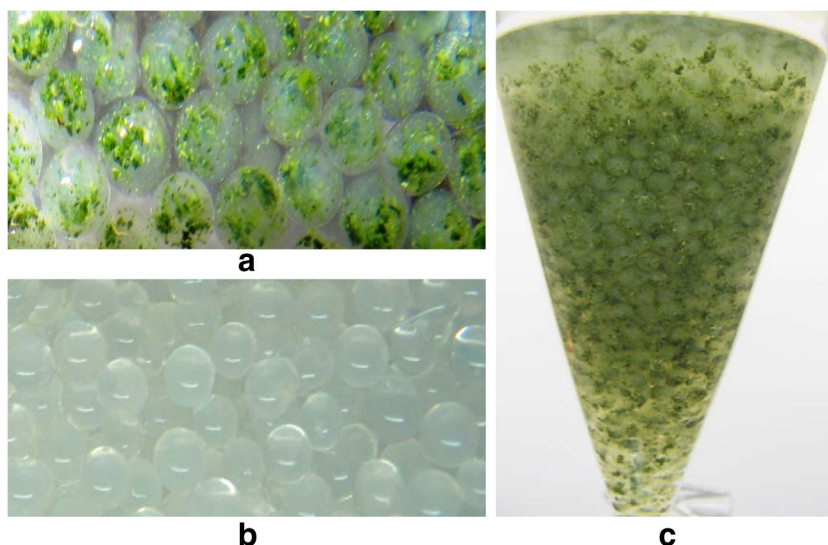
process of lithium ions biosorption were alkanes, phenolic, and amide groups.

### Scanning electron microscopy

SEM images have clearly shown that *Oocystis solitaria* samples before and after lithium biosorption showed different surface morphologies. *Oocystis solitaria* biomass before adsorption of lithium ions (Fig. 4a) displays a uniformly interconnected structure with a continuous surface. While after lithium biosorption by *Oocystis solitaria* biomass (Fig. 4b), biomass walls became fragile with irregular surfaces and the appearance of bright spots, indicating the ability of *Oocystis solitaria* biomass to remove lithium from aqueous solutions.



**Fig. 5** Immobilization of *Oocystis solitaria* in alginate beads and its application in lithium ions removal from aqueous solution. **a** Sodium alginate–*Oocystis solitaria* beads. **b** Sodium alginate beads without incorporation of the algal biomass. **c** Separating funnel packed with alginate–algal beads



### Immobilization of *Oocystis solitaria* cells in alginate beads and its application in lithium removal

The ability of immobilized *Oocystis solitaria* (in sodium alginate beads) to remove lithium from aqueous solution has been studied (Fig. 5), and the results were presented in Fig. S2. The results indicated that 98.71% of the lithium was removed after treatment of aqueous solution containing 200 mg/L lithium with immobilized *Oocystis solitaria* cells after 5 h, which is significantly higher than the removal that was obtained by using sodium alginate beads without merging the biomass of alga as a control (90.19%) (Fig. S2). Some studies have reported that immobilized cells have higher efficiency in metal absorption than the free cells (Mallick 2002; Rangsayatorn et al. 2004; Gadd 2009; Barquilha et al. 2017). The size of beads used to immobilize biomass is a significant factor (Mehta and Gaur 2005). The beads can be used in successive biosorption cycles to remove the metal ions from the aqueous solutions, indicating that immobilization can provide an effective and suitable technique for the repeated use of the biosorbent (Ahmad et al. 2017).

### Conclusion

Biosorption of heavy metals by natural materials provide potential alternative and promising technology to overcome the disadvantages of conventional methods to remove metal ions from aqueous solutions and wastewater. The results of the proposed technique indicate that lithium can be removed effectively from water using immobilized unicellular green alga, *Oocystis solitaria*, cells in sodium alginate beads. Therefore, *Oocystis solitaria* can be used as an alternative for sorption and removal of lithium ions from wastewaters. Our study recommends that the study should continue to include the

unicellular green alga, *Oocystis solitaria*, in a biologically inert matrix which may be used in bead forms ingested orally to remove lithium from biological fluids, e.g., gastrointestinal fluids.

**Authors' contributions** NEE designed the experiments and experimental instructions, performed the statistical analysis, analyzed and interpreted the data, and contributed substantially to the writing and revising of the manuscript. RAH proposed the research concept, providing necessary tools for the experiments and experimental instructions; contributed to the manuscript reviewing; and had given the final approval of the version to be published. IEM performed the lithium ions analysis using inductively coupled plasma atomic emission spectroscopy (ICP-AES) (Thermo Scientific). MSA provided some necessary tools for experiments and had given the final approval of the version to be published. NHR carried out the experiments and contributed substantially to the writing of the manuscript. All authors read and approved the final manuscript.

### Compliance with ethical standards

**Conflict of interest** The authors declare that they have no competing interests.

### References

- Ahmad A, Bhat AH, Buang A (2017) Biosorption of transition metals by freely suspended and Ca-alginate immobilized with *Chlorella vulgaris*: kinetic and equilibrium modeling. *J Clean Prod* 171: 1361–1375
- Ahmaruzzaman M, Gupta VK (2011) Rice husk and its ash as low-cost adsorbents in water and waste water treatment. *Ind Eng Chem Res* 50:13589–13613
- Ajayan KV, Selvaraju M, Thirugnanamoorthy K (2011) Growth and heavy metals accumulation potential of microalgae grown in sewage wastewater and petrochemical effluents. *Pak J Biol Sci* 14:805–811
- Al-Ashed S, Duvnjak Z (1995) Adsorption of copper and chromium by *Aspergillus carbonarius*. *Biotechnol Prog* 11:638–642
- Alok M, Jyoti M, Arti M, Gupta VK (2010) Removal and recovery of chrysoidine Y from aqueous solutions by waste materials. *J Colloid Interface Sci* 344:497–507

- American Public Health Association (APHA) (2005) Standard methods for the examination of water and wastewater, 22nd edn. APHA, Inc, Washington, D.C.
- Andersen RA (ed) (2005) Algal culturing techniques. Elsevier Academic Press, New York, 578 p
- Aral H, Vecchio-Sadus A (2008) Toxicity of lithium to humans and the environment—a literature review. *Ecotoxicol Environ Saf* 70:349–356
- Aravindhan R, Fathima NN, Rao JR, Nair BU (2007) Equilibrium and thermodynamic studies on the removal of basic black dye using calcium alginate beads. *Colloids Surf A Physicochem Eng Asp* 299:232–238
- Banik RM, Santhiagu A, Upadhyay SN (2007) Optimization of nutrients for gellan gum production by *Sphingomonas paucimobilis* ATCC-31461 in molasses based medium using response surface methodology. *Bioresour Technol* 98:792–797
- Barquilha CER, Cossich ES, Tavares CRG, Silva EA (2017) Biosorption of nickel(II) and copper(II) ions in batch and fixed-bed columns by free and immobilized marine algae *Sargassum* sp. *J Clean Prod* 150: 58–64
- Becker RW, Tyobeka EM (1990) Lithium enhances proliferation of HL60 promyelocytic leukemia cells. *Leuk Res* 14:879–884
- Birch NJ (1988) Lithium. In: Seiler HG, Sigel H, Sigel A (eds) Handbook on the toxicity of inorganic compounds. Marcel Dekker, New York, pp 382–393
- Box GEP, Behnken DW (1960) Some new three level designs for the study of quantitative variables. *Technometrics* 2:455–475
- Box GEP, Hunter WG, Hunter JS (1978) Statistics for experimenters. John Wiley & Sons, New York
- Chang CY, Lee CL, Pan TM (2006) Statistical optimization of medium components for the production of *Antrodia cinnamomea* AC0623 in submerged cultures. *Appl Microbiol Biotechnol* 72:654–661
- Chassard-Bouchaud C, Galle P, Escaig F, Miyawaki M (1984) Bioaccumulation of lithium by marine organisms in European, American, and Asian coastal zones: microanalytic study using secondary ion emission. *Comptes Rendus de l'Académie des Sciences, Série III* 299(18):719–724
- Choudhary DK, Sharma KP, Gaur RK (2011) Biotechnological perspectives of microbes in agro-ecosystems. *Biotechnol Lett* 33: 1905–1910
- Çicek A, Yilmaz O, Arar O (2018) Removal of lithium from water by aminomethyl phosphonic acid-containing resin. *J Serb Chem Soc* 83:1059–1069
- Cui L, Ouyang Y, Lou Q, Yang F, Chen Y, Zhu W, Luo S (2009) Removal of nutrients from wastewater with *Canna indica* L. under different vertical-flow constructed wetland conditions. *Ecol Eng* 36:1083–1088
- Dadrasnia A, Ismail S (2015) Biosurfactant production by *Bacillus salmalaya* for lubricating oil solubilization and biodegradation. *Int J Environ Res Public Health* 12:9848–9863
- Devi TSR, Gayathri S (2010) FTIR and FT-Raman spectral analysis of paclitaxel drugs. *Int J Pharm Sci Rev Res* 2(2):106–110
- El-Naggar NE (2015) Extracellular production of the oncolytic enzyme, L-asparaginase, by newly isolated *Streptomyces* sp. strain NEAE-95 as potential microbial cell factories: optimization of culture conditions using response surface methodology. *Curr Pharm Biotechnol* 16(2):162–178
- El-Naggar NE, El-Bindary AA, Nour NS (2013) Statistical optimization of process variables for antimicrobial metabolites production by *Streptomyces anulatus* NEAE-94 against some multidrug-resistant strains. *Int J Pharm* 9:322–334
- El-Naggar NE, Hamouda RA, Mousa IE, Abdel-Hamid MS, Rabei NH (2018a) Statistical optimization for cadmium removal using *Ulva fasciata* biomass: characterization, immobilization and application for almost-complete cadmium removal from aqueous solutions. *Sci Rep* 8:12456
- El-Naggar NE, Hamouda RA, Mousa IE, Abdel-Hamid MS, Rabei NH (2018b) Biosorption optimization, characterization, immobilization and application of *Gelidium amansii* biomass for complete Pb<sup>2+</sup> removal from aqueous solutions. *Sci Rep* 8:13456
- El-Sikaily A, El Nemr A, Khaled A, Abdelwehab O (2007) Removal of toxic chromium from wastewater using green alga *Ulva lactuca* and its activated carbon. *J Hazard Mater* 148:216–228
- Esmaili A, Beni AA (2015) Biosorption of nickel and cobalt from plant effluent by *Sargassum glaucescens* nanoparticles at new membrane reactor. *Int J Environ Sci Technol* 12:2055–2064
- Furr AK (2000) CRC handbook of laboratory safety. CRC, Boca Raton, pp 244–246
- Gadd GM (2009) Biosorption: critical review of scientific rationale, environmental importance and significance for pollution treatment. *J Chem Technol Biotechnol* 84:13–28
- Garg U, Kaur MP, Jawa GK, Sud D, Garg VK (2008) Removal of cadmium (II) from aqueous solutions by adsorption on agricultural waste biomass. *J Hazard Mater* 154:1149–1157
- Ghaedi M, Hajjati S, Mahmudi Z, Tyagi I, Agarwal S, Maity A, Gupta VK (2015) Modeling of competitive ultrasonic assisted removal of the dyes—methylene blue and Safranin-O using Fe<sub>3</sub>O<sub>4</sub> nanoparticles. *Chem Eng J* 268:28–37
- Ghosh MK, Mittal KL (eds) (1996) Polyimides: fundamentals and applications. Marcel Dekker, New York
- Grandjean EM, Aubry JM (2009) Lithium: updated human knowledge using an evidence-based approach: part I: clinical efficacy in bipolar disorder. *CNS Drugs* 23:225–240
- Greasham R, Inamine E (1986) Nutritional improvement of processes. In: Demain AL, Soloman LA (eds) Manual of industrial microbiology and biotechnology. American Society for Microbiology; Nutritional improvement of process, Washington, DC, USA, pp 41–48
- Gunasekaran S, Abitha P (2005) Fourier transform infrared and FT-Raman spectra and normal coordinate analysis of aminobenzoic acid. *Indian J Pure Appl Phys* 43:329–334
- Gupta VK, Rastogi A (2008) Biosorption of lead from aqueous solutions by green algae *Spirogyra* species: kinetics and equilibrium studies. *J Hazard Mater* 152:407–414
- Gupta VK, Saleh TA (2013) Sorption of pollutants by porous carbon, carbon nanotubes and fullerene—an overview. *Environ Sci Pollut Res* 20:2828–2843
- Gupta VK, Nayak A, Agarwal S (2015) Bioadsorbents for remediation of heavy metals: Current status and their future prospects. *Environ Eng Res* 20: 1–18
- Gupta VK, Sharma S, Yadav IS, Mohan D (1998) Utilization of bagasse fly ash generated in the sugar industry for the removal and recovery of phenol and *p* nitrophenol from wastewater. *J Chem Technol Biotechnol* 71:180–186
- Gupta VK, Jain R, Nayak A, Agarwal S, Shrivastava M (2011) Removal of the hazardous dye—tartrazine by photodegradation on titanium dioxide surface. *Mater Sci Eng C* 31:1062–1067
- Gupta VK, Ali I, Saleh TA, Siddiqui MN, Agarwal S (2013) Chromium removal from water by activated carbon developed from waste rubber tires. *Environ Sci Pollut Res* 20:1261–1268
- Gupta VK, Atar N, Yola ML, Üstündağ Z, Uzun L (2014a) A novel magnetic Fe@Au core-shell nanoparticles anchored graphene oxide recyclable nanocatalyst for the reduction of nitrophenol compounds. *Water Res* 48:210–217
- Gupta VK, Nayak A, Agarwal A, Tyagi I (2014b) Potential of activated carbon from waste rubber tire for the adsorption of phenolics: effect of pre-treatment conditions. *J Colloid Interface Sci* 417:420–430
- Hassan AF, Abdel-Mohsen AM, Fouda MMG (2014) Comparative study of calcium alginate, activated carbon, and their composite beads on methylene blue adsorption. *Carbohydr Polym* 102:192–198
- Ho Y-S, Chiang C-C, Hsu Y-C (2001) Sorption kinetics for dye removal from aqueous solution using activated clay. *Sep Sci Technol* 36: 2473–2488

- Hudson RL, Moore MH (2000) IR spectra of irradiated cometary ice analogues containing methanol: a new assignment, a reassignment, and a nonassignment. *Icarus* 145:661–663
- Ibrahim WM (2011) Biosorption of heavy metal ions from aqueous solution by red macroalgae. *J Hazard Mater* 192:1827–1835
- Jackson P, Robinson K, Puxty G, Attalla M (2009) In situ Fourier transform-infrared (FT-IR) analysis of carbon dioxide absorption and desorption in amine solutions. *Energy Procedia* 1(1):985–994
- Janakiraman N, Johnson M (2015) Functional groups of tree ferns (CYATHEA) using FT-IR: chemotaxonomic implications. *Romanian J Biophys* 25:131–141
- Kaneko S, Takahashi W (1990) Adsorption of lithium in seawater on alumina-magnesia mixed-oxide gels. *Colloids Surf A Physicochem Eng Asp* 47:69–79
- Kastanek P, Ferreira P, Kastanek F, Prochazkova G, Jandova J, Kronusova O, Solcova O, Rouskova M (2015) Recovery and bioaccumulation of lithium and rubidium from diluted aqueous waste leachates by microalgae. *Proceedings of the 14th International Conference on Environmental Science and Technology Rhodes, Greece, 3–5 September*
- Kato T, Fujii K, Shiori T, Inubushi T, Takahashi S (1996) Lithium side effects in relation to brain lithium concentration measured by lithium-7 magnetic resonance spectroscopy. *Prog Neuro-Psychopharmacol Biol Psychiat* 20:87–97
- Khani H, Rofouei MK, Arab P, Vinod Kumar Gupta VK, Vafaei Z (2010) Multi-walled carbon nanotubes-ionic liquid-carbon paste electrode as a super selectivity sensor: application to potentiometric monitoring of mercury ion(II). *J Hazard Mater* 183:402–409
- Kjølholt J, Stuer-Lauridsen F, Skibsted Mogensen A, Havelund S (2003) The elements in the second rank—lithium. *Miljøministeriet, Copenhagen, Denmark*
- Klug S, Collins M, Nagao T, Merker HJ, Neubert D (1992) Effect of lithium on rat embryos in culture: growth, development, compartmental distribution and lack of a protective effect of inositol. *Arch Toxicol* 66:719–728
- Kudre TG, Bhaskar N, Sakhare PZ (2017) Optimization and characterization of biodiesel production from rohu (*Labeo rohita*) processing waste. *Renew Energy* 113:1408–1418
- Kumar SS, Saramma AV (2012) Nitrate and phosphate uptake by immobilized cells of *Gloeocapsa gelatinosa*. *J Mar Biol Assoc India* 54:119–122
- Kumar YP, King P, Prasad VSRK (2006) Removal of copper from aqueous solution using *Ulva fasciata* sp. a marine green alga. *J Hazard Mater* 137:367–373
- Kumar M, Pal A, Singh J, Garg S, Bala M, Vyas A, Khasa YP, Pachour UC (2013) Removal of chromium from water effluent by adsorption onto *Vetiveria zizanioides* and *Anabaena* species. *Nat Sci* 5:341–348
- Kuznetsov IA, Lukanin AS, Tsurkanov LF (1971) Effect of ions of the alkaline metals on the secondary structure of DNA. IV Thermal denaturing deoxyribonucleates of alkaline metals in solution with a low ionic strength. *Biofizika* 16:144–145
- Léonard A, Hantson P, Gerber GB (1995) Mutagenicity, carcinogenicity teratogenicity of lithium compounds. *Mutat Res Rev Genet Toxicol* 339(3):131–137
- Li PS, Tao HC (2015) Cell surface engineering of microorganisms towards adsorption of heavy metals. *Crit Rev Microbiol* 41:140–149
- Li SY, Zou DH, Luo YW, Sun QR, Deng KF, Chen YJ, Huang P (2014) Characteristics of electrically injured skin from human hand tissue samples using Fourier transform infrared microspectroscopy. *Sci Justice* 54:98–104
- Lian L, Guo L, Guo C (2009) Adsorption of Congo red from aqueous solution on Ca-bentonite. *J Hazard Mater* 161:126–131
- Litovitz TL, Clark LR, Soloway RA (1994) Annual report of the American Association of Poison Control Centers toxic exposure surveillance system. *Am J Emerg Med* 12(5):546–548
- Mallick N (2002) Biotechnological potential of immobilized algae for wastewater N, P and metal removal: a review. *Biometals* 15:377–390
- Meena AK, Mishra GK, Rai PK, Rajagopal C, Nagar PN (2005) Removal of heavy metals ions from aqueous solution using carbon aerogel as an adsorbent. *J Hazard Mater* 122:161–170
- Mehta SK, Gaur JP (2005) Use of algae for removing heavy metal ions from wastewater: progress and prospects. *Crit Rev Biotechnol* 25:113–152
- Miyai Y, Kanoh H, Feng Q, Ooi K (1978) Intraparticle diffusion coefficient of lithium on granulated adsorbent of manganese oxide in seawater. *Nippon Kaisui Gakkai-Shi Bulletin NKAGBU* 49:347–351
- Mohammadi N, Khani H, Gupta VK, Amereh E, Agarwal S (2011) Adsorption process of methyl orange dye onto mesoporous carbon material—kinetic and thermodynamic studies. *J Colloid Interface Sci* 362:457–462
- Momcilovic M, Purenovic M, Bojic A, Zarubica A, Randelovic M (2011) Removal of lead(II) ions from aqueous solutions by adsorption onto pine cone activated carbon. *Desalination* 276:53–59
- Nawani NN, Kapadnis B (2005) Optimization of chitinase production using statistic based experimental designs. *Process Biochem* 40:651–660
- Pagnanelli F, Esposito A, Toro L, Veglio F (2003) Metal speciation and pH effect on Pb, Cu, Zn and Cd biosorption onto *Sphaerotilus natans*: Langmuir-type empirical model. *Water Res* 37:627–633
- Park D, Yun YS, Park JM (2010) The past, present, and future trends of biosorption. *Biotechnol Bioproc E* 15:86–102
- Philipose MT (1967) Chlorococcales, vol 8. *Indian Council of Agricultural Research, New Delhi, India*, pp 31–41
- Plackett RL, Burman JP (1946) The design of optimum multifactorial experiments. *Biometrika* 33:305–325
- Popper ZA, Michel G, Herve C, Domozych DS, Willats WG, Tuohy MG, Kloareg B, Stengel DB (2011) Evolution and diversity of plant cell walls: from algae to flowering plants. *Annu Rev Plant Biol* 62:567–590
- Priyadarshani I, Sahu D, Rath B (2011) Microalgal bioremediation: current practices and perspectives. *J Biochem Technol* 3:299–304
- Rangsayatorn N, Pokethitiyook P, Upatham ES, Lanza GR (2004) Cadmium biosorption by cells of *Spirulina platensis* TISTR 8217 immobilized in alginate and silica gel. *Environ Int* 30:57–63
- Reddad Z, Gerente C, Andres Y, Cloirec PL (2002) Adsorption of several metal ions onto a low-cost biosorbent: kinetic and equilibrium studies. *Environ Sci Technol* 36:2067–2073
- Rippka R, Deruelles J, Waterbury JB, Herdman M, Stanier RY (1979) Generic assignments, strain histories and properties of pure cultures of cyanobacteria. *J Gen Microbiol* 111:1–61
- Romera E, Gonzalez F, Ballester A, Blazquez ML, Munoz JA (2007) Comparative study of heavy metals using different types of algae. *Bioresour Technol* 98:3344–3353
- Saleem M, Pirzada T, Qadeer R (2007) Sorption of acid violet 17 and direct red 80 dyes on cotton fiber from aqueous solutions. *Colloids Surf A Physicochem Eng Asp* 292:246–250
- Saleh TA, Gupta VK (2011) Functionalization of tungsten oxide into MWCNT and its application for sunlight-induced degradation of rhodamine B. *J Colloid Interface Sci* 362:337–344
- Saleh TA, Gupta VK (2012) Photo-catalyzed degradation of hazardous dye methyl orange by use of a composite catalyst consisting of multi-walled carbon nanotubes and titanium dioxide. *J Colloid Interface Sci* 371:101–106
- Salem AMS, Harraz FA, El-Sheikh SM, Hafez HS, Ibrahima IA, Abdel-Mottaleb MSA (2015) Enhanced electrical and luminescent performance of porous silicon/MEH-PPV nanohybrid synthesized by anodization and repeated spin coating. *RSC Adv* 5:99892–99898
- Saravanan R, Karthikeyan S, Gupta VK, Sekaran G, Narayanan V, Stephen A (2013a) Enhanced photocatalytic activity of ZnO/CuO



- nanocomposite for the degradation of textile dye on visible light illumination. *Mater Sci Eng C* 33:91–98
- Saravanan R, Thirumal E, Gupta VK, Narayanan V, Stephen A (2013b) The photocatalytic activity of ZnO prepared by simple thermal decomposition method at various temperatures. *J Mol Liq* 177:394–401
- Saravanan R, Gupta VK, Prakash T, Narayanan V, Stephen A (2013c) Synthesis, characterization and photocatalytic activity of novel Hg doped ZnO nanorods prepared by thermal decomposition method. *J Mol Liq* 178:88–93
- Saravanan R, Karthikeyan N, Gupta VK, Thirumal E, Thangadurai P, Narayanan V, Stephen A (2013d) ZnO/Ag nanocomposite: an efficient catalyst for degradation studies of textile effluents under visible light. *Mater Sci Eng C* 33:2235–2244
- Saravanan R, Joicy S, Gupta VK, Narayanan V, Stephen A (2013e) Visible light induced degradation of methylene blue using CeO<sub>2</sub>/V<sub>2</sub>O<sub>5</sub> and CeO<sub>2</sub>/CuO catalysts. *Mater Sci Eng C* 33:4725–4731
- Saravanan R, Gupta VK, Narayanan V, Stephen A (2013f) Comparative study on photocatalytic activity of ZnO prepared by different methods. *J Mol Liq* 181:133–141
- Saravanan R, Gupta VK, Narayanan V, Stephen A (2014a) Visible light degradation of textile effluent using novel catalyst ZnO/g-Mn<sub>2</sub>O<sub>3</sub>. *J Taiwan Inst Chem Eng* 45:1910–1917
- Saravanan R, Gupta VK, Mosquera E, Gracia F (2014b) Preparation and characterization of V<sub>2</sub>O<sub>5</sub>/ZnO nanocomposite system for photocatalytic application. *J Mol Liq* 198:409–412
- Saravanan R, Mansoob Khan M, Gupta VK, Mosquera E, Gracia F, Narayanan V, Stephen A (2015) ZnO/Ag/Mn<sub>2</sub>O<sub>3</sub> nanocomposite for visible light induced industrial textile effluent degradation, uric acid and ascorbic acid sensing and antimicrobial activity. *RSC Adv* 5:34645–34651
- Staniszewska-Slezak E, Fedorowicz A, Kramkowski K, Leszczynska A, Chlopicki S, Baranska M, Malek K (2015) Plasma biomarkers of pulmonary hypertension identified by Fourier transform infrared spectroscopy and principal component analysis. *Analyst* 140:2273–2279
- Tsuruta T (2005) Removal and recovery of lithium using various microorganisms. *J Biosci Bioeng* 100:562–566
- Van de Voort FR, Sedman J, Cocciardi R, Juneau S (2007) An automated FTIR method for the routine quantitative determination of moisture in lubricants: an alternative to Karl Fischer titration. *Talanta* 72:289–295
- Vijayaraghavan K, Yun YS (2008) Bacterial biosorbents and biosorption. *Biotechnol Adv* 26:266–291
- Volesky B (2003) Sorption and biosorption, first edn. BV Sorbex, Inc., Quebec, Canada
- Wedepohl KH (1995) The composition of the continental crust. *Geochim Cosmochim Acta* 59:1217–1232
- Zahariev I, Piskin M, Karaduman E, Ivanova D, Markova I, Fachikov L (2017) FTIR spectroscopy method for investigation of Co-Ni nanoparticle nanosurface phenomena. *J Chem Technol Metallurgy* 52:916–928

**Publisher's note** Springer Nature remains neutral with regard to jurisdictional claims in published maps and institutional affiliations.